Processing and properties of centimeter-long, in-fiber, crystalline-selenium filaments

D. S. Deng,[1,2] N. D. Orf,[1,2] S. Danto,[1] A. F. Abouraddy,[1,a)] J. D. Joannopoulos,[3] and Y. Fink[1,2,b)]
[1]*Research Laboratory of Electronics, Massachusetts Institute of Technology, 77 Massachusetts Avenue, Cambridge, Massachusetts 02139, USA*
[2]*Department of Materials Science and Engineering, Massachusetts Institute of Technology, 77 Massachusetts Avenue, Cambridge, Massachusetts 02139, USA*
[3]*Department of Physics, Massachusetts Institute of Technology, 77 Massachusetts Avenue, Cambridge, Massachusetts 02139, USA*

(Received 25 September 2009; accepted 30 November 2009; published online 11 January 2010)

We report on the fabrication and characterization of globally ordered crystalline selenium filaments with diameters about 200 nm and aspect ratios upwards of 10^5. Amorphous Se filaments are fabricated by a recently developed approach in which a thin film evolves into an ordered array of filaments in fiber. Single-crystal and polycrystalline filaments are attained with a postdrawing annealing procedure. Arrays of two-cm-long crystalline nanowires, electrically contacted to external circuitry through the fiber end facets, exhibit a two-orders-of-magnitude change in conductivity between dark and illuminated states. These results hold promise for the fabrication of filament-detector arrays that may be integrated with large-area electronics. © *2010 American Institute of Physics*. [doi:10.1063/1.3275751]

Interest in efficient processing of crystalline semiconductor filaments of submicron dimensions is motivated by their unique physical properties[1] and potential for a wide range of applications.[2–5] Vapor-liquid-solid (VLS) growth has emerged as an important method for the fabrication of high-quality filaments.[6] Nevertheless, filaments produced by the conventional VLS approach are inherently limited to micrometer-length scales, are fraught with mechanical fragility, and lack global orientation. Several attempts have been made to embed crystalline submicron filaments into optical fibers with a number of different methods including high-pressure chemical vapor deposition,[7] pumping-and-filling techniques,[8] or the multiple-step, draw-cut-stack approach.[9,10] While combining crystalline filaments with optical fibers has generated much interest, several challenges to producing nanowires using thermal drawing remain, a consequence of the orders-of-magnitude disparity between typical fiber and filament dimensions. Moreover, the above described approaches do not take full advantage of the fundamental simplicity of the traditional fiber thermal-drawing process which is, nevertheless, at odds with the desire to produce crystalline structures.

To fabricate extended crystalline semiconductor filaments, we implement a one-step, optical-fiber codrawing process which is based on an intriguing fluid-instability phenomenon whereby a viscous semiconductor film spontaneously evolves into a periodic array of amorphous filaments as its thickness is reduced [Fig. 1(a)].[11] A macroscopic eight-centimeter-long preform is constructed by first thermally depositing a semiconductor (selenium) film onto a thick polymer (polysulfone, PSU) film, wrapping the composite film along with additional polymer sheets around a mandrel and then finally fusing the layers into a single solid structure [Fig. 1(b)]. The completed preform (a composite of PSU and Se) is heated until it becomes viscous (at approximately 260 °C) and is then controllably drawn down into an extended tens-of-meters-long fiber by the application of uniaxial tension [Fig. 1(c)]. When the thickness of the Se thin film in the initial preform drops below a characteristic length scale, determined by the viscosity of the two materials and their surface energy,[11] the film spontaneously breaks up into an ordered array of filaments in the final fiber.

This process has several unique advantages. First, the filaments have unprecedented length, in principle extending along the entire tens-of-meters-long fiber. Second, the process aligns all the filaments with the same global orientation. Third, the mechanically tough polymer matrix hermetically seals the nanowires into a structure that may be macroscopically manipulated, hence bypassing the problems associated

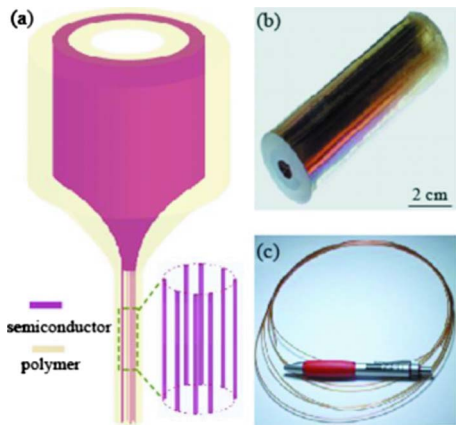

FIG. 1. (Color online) Fabrication of filament arrays using optical-fiber thermal drawing technique. (a) Schematic diagram of break-up of a thin cylindrical shell into a periodic array of filaments. During thermal drawing, a macroscopic preform is heated to the viscous state and controllably stretched into an extended fiber. [(b) and (c)] Photographs of a 8-cm-long preform and of several meters of fiber, respectively.

a)Present address: CREOL, The College of Optics & Photonics, 4000 Central Florida Blvd., Orlando, Florida, 32816 (USA).
b)Electronic mail: yoel@mit.edu.

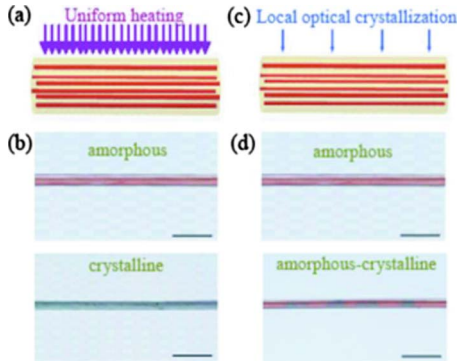

FIG. 2. (Color online) Thermal and optical crystallization of fiber-embedded selenium filaments. (a) Schematic diagram of thermal annealing and (b) photographs highlighting the visible change from brick red (amorphous filaments, upper photograph) to gray(crystalline filaments, lower photograph) corresponding to the amorphous/crystalline transition brought about by annealing. (c) Schematic diagram of laser-induced local crystallization and (d) photographs of a fiber with alternating amorphous (brick-red) and crystalline (gray) regions along the fiber axis. Scale bar in all of the photographs is 1 cm.

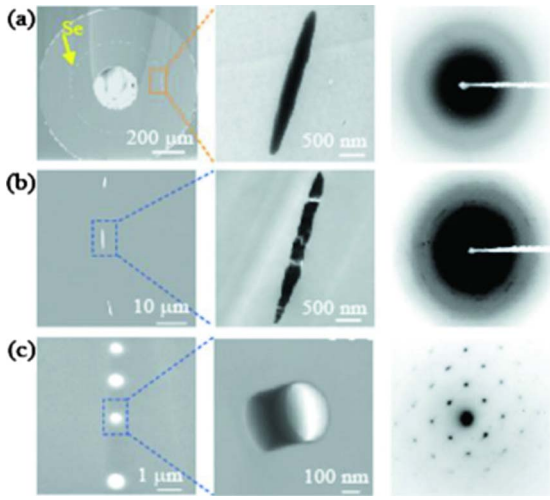

FIG. 3. (Color online) Filament characterization. (a) Amorphous filament arrays. Left, an SEM micrograph of a fiber cross-section containing a filament array; middle, TEM micrographs and, right, corresponding electron diffraction patterns of *a*-Se filaments resulting from an initial 2 μm thick continuous amorphous film. (b) Polycrystalline filament arrays. Left, a magnified SEM micrograph of ellipsoidal filaments; middle, TEM micrograph; right, electron diffraction pattern demonstrating polycrystallinity. (c) Crystalline filament array. Left, a magnified SEM micrograph of a filament array resulting from the complete break up of a continuous amorphous film having an initial 200 nm thickness; middle, TEM micrograph, and, right, single crystal electron diffraction pattern.

with the mechanical fragility of nanostructures. Additionally, the approach is compatible with a variety of materials including metals (Sn, Bi) and semiconductors (As_2Se_3, As_2S_3, Se).

Crystalline selenium (c-Se) filaments are attained by a postdrawing annealing process.[12] Upon exiting the drawing furnace the selenium filaments rapidly cool and are quenched into the amorphous state. As selenium is an unstable glass and can easily go between the amorphous and crystalline states,[13] the filaments may be converted to the equilibrium crystalline state simply by annealing at 150 °C for 1 h [Fig. 2(a)]. This temperature is substantially below the glass transition of the polymer cladding (polysulfone, $T_g \sim 190$ °C), and the polymer is therefore unaffected by the annealing.[14] The transition of the filaments embedded in the fiber from the amorphous state to the crystalline state can be readily discerned visually from the dramatic change in filament color. Figure 2(b) (top panel) shows a filament-embedded fiber section having brick-red color (light gray in print) characteristic of amorphous selenium. Upon annealing, the filament color changes into a dark gray [Fig. 2(b), bottom panel]. Crystallization of the filaments may also be induced optically by illuminating sections of the same fiber for 2 h with a 532 nm laser [Fig. 2(c)]. The laser power density was kept below 10 mW/cm^2 in order to minimize heating effects.[15] An optical micrograph of a four-period structure of alternating amorphous and crystalline domains obtained in this way is shown in Fig. 2(d).

After presenting macroscopic-scale evidence for amorphous/crystalline phase transitions in the ensemble of fiber-encased filaments both thermally and optically, we proceed to demonstrate this phase transition at the single-filament level. This allows us, in particular, to quantitatively determine the extent of crystallization that the filaments undergo. The transition between the amorphous and crystalline phases was confirmed by transmission electron microscopy (TEM) and diffraction measurements performed on the fiber cross-sections. A SEM micrograph [Fig. 3(a) left] shows a fiber cross-section with an array of filaments having elliptical cross-sections arising from the breakup of a 2 μm film after its thickness was reduced by a factor of 20 vis-à-vis thermal drawing. A TEM cross-section of an individual Se filament prior to annealing is shown in Fig. 3(a) (middle). A TEM diffraction pattern [Fig. 3(a) right] shows only diffuse halos indicative of an amorphous phase. After annealing, multiple grain boundaries are seen in the TEM image [Fig. 3(b) middle], and the electron diffraction pattern [Fig. 3(b) right] shows satellite spots in concentric rings indicating polycrystallinity.

In light of the typical grain sizes observed in the annealed filaments, it is expected that nearly single-crystal filaments will be obtained when the filament size decreases below this average grain size. To verify this, a preform containing a 200 nm selenium film was drawn into fiber with the intention of reducing the film thickness to 10 nm. The SEM and TEM micrographs in Fig. 3(c) (left) and (middle), respectively, show the film has broken up into filaments having circular cross-sections and an average spacing between filaments (i.e., the instability wavelength, λ) of approximately 3 μm. A diffraction pattern taken from one of these filaments [Fig. 3(c) right] demonstrates the single-crystalline nature of the filament sample, thus confirming the above thesis.

A simple estimate of the filament diameter can be obtained by conservation of volume arguments. The area of the actual filament cross-section can be equated to the initial thickness of the film divided by the draw-down ratio (which would be the film thickness in the fiber in the absence of break-up) times the distance between filaments λ,

$$\pi D^2/4 \sim \lambda(h/z),$$

where D is the filament diameter, h is the initial semiconductor layer thickness, z is the preform-to-fiber draw-down ratio, and λ is the instability wavelength. The initial film thickness of the fiber depicted in Fig. 3(c) was 200 nm and the fiber was drawn-down by a factor of 20. Thus, as $h/z \sim 200/20$ nm and $\lambda \sim 3$ μm, the filament diameter is estimated to be approximately 200 nm, close to the actual filament size [Fig. 3(c) middle]. The ultimate filament diameter is determined by the initial film thickness, the viscosity, and

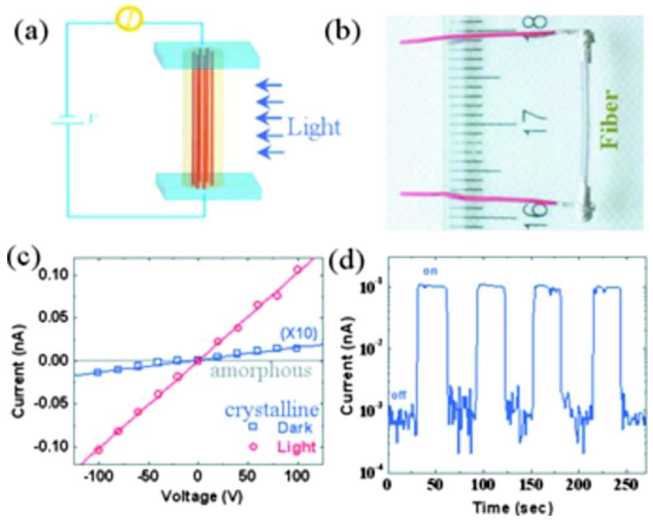

FIG. 4. (Color online) Electrical connection and optoelectronic properties of centimeter-long c-Se filaments. [(a) and (b)] Sketch and photograph of electrical contact to an external circuit by connecting the fiber end facets. (c) Current-voltage characteristics of an array of 2-cm-long c-Se filaments in the dark (open squares) and under illumination (open circles). No detectable current was observed in the *a*-Se filaments (solid line), owing to their large resistivity. (d) Reversible switching between high and low photoconductivity states as the externally incident illumination is modulated.

surface tension of the materials used, and the draw-down ratio. Using this same technique, amorphous As_2Se_3 filaments have been drawn to thicknesses less than 20 nm.[11]

Lastly, we demonstrate an in-fiber crystalline-filament device in the form of a photodetector or optical switch. In contrast to many other nanowire arrays, the entire fiber filament array can be easily connected to external circuitry by contacting the two fiber ends with a conductor [schematic in Fig. 4(a)]. For example, an in-fiber array of polycrystalline filaments was contacted by applying silver paint to both ends of a fiber segment and then wrapping thin metal wire around the silver-painted ends [Fig. 4(b)]. A number of 2-cm-long filament arrays were cut out of the original 20-m-long fiber and measured. These sections displayed similar ohmic characteristics under applied bias [Fig. 4(c)] and the electrical conductivity of the filaments in the dark can be estimated from the applied voltage, measured current, and array dimensions. The calculated conductivity of 10^{-8} Ω^{-1} cm^{-1} is less than that of bulk single crystal selenium ($\sim 10^{-6}$ Ω^{-1} cm^{-1}).[16] Significant disparities in conductivity between filaments and the bulk have been observed previously and have been attributed to enhanced inelastic scattering of carriers at surfaces due to increased surface-to-volume ratios, reflection of electrons at grain boundaries, and defects or impurities along the high aspect ratio wires.[17] An array of amorphous filaments was contacted and measured in the same way [solid line in Fig. 4(c)] but no current was recorded owing to its extremely low conductivity ($<10^{-16}$ Ω^{-1} cm^{-1}).[18] The measurable current of the c-Se filament arrays confirms that there is a continuous path between fiber ends and that the selenium filaments are at least 2 cm in length.

The filament arrays exhibit enhanced photoconductivity under illumination from a 500 mW/cm^2 broadband white-light source [open circles in Fig. 4(c)]. A repeatable two-orders-of-magnitude change in current is demonstrated by turning the illumination on and off under fixed applied bias [Fig. 4(d)]. The observed fluctuation of dark current may be due to thermal and generation-recombination noise. The large difference in light and dark conductivity suggests possible use as an optical switch. Unlike other nanowire devices,[19] the photoconductivity of the filament arrays is unaffected by changes in the local environment due to contamination or humidity, as they are clad in the polymer matrix.

The simplicity of electrical contact to the filament arrays by directly connecting fiber end facets is a result of the fabrication method. The filaments themselves are generated in a unidirectional process, imparting a completely uniform global orientation. The polymer matrix forms a protective and mechanically tough sheath that enables simple and macroscopic manipulation to be carried out in a straightforward fashion without expensive nanomanipulation techniques, circumventing a major challenge to the large-scale integration of filament devices.

In summary, we demonstrate a technique to fabricate, manipulate, and electronically address one-dimensional crystalline semiconductor filament arrays. The optical fiber drawing technique enables very long lengths of continuous and aligned filaments to be generated in a straightforward fashion. Moreover, the process of laser-induced local crystallization is similar to the read/write process in phase-change materials,[20] and the filaments themselves may become a unique data storage platform.

We acknowledge H. Stone for fruitful discussions. This work was supported by ARO ISN under Contract No W911NF-07-D-0004, and the MRSEC program of NSF under award number DMR-0819762.

[1] Y. N. Xia, P. D. Yang, Y. Sun, Y. Wu, B. Mayers, B. Gates, Y. Yin, F. Kim, and H. Yan, Adv. Mater. **15**, 353 (2003).
[2] Y. Cui, Z. H. Zhong, D. L. Wang, W. U. Wang, and C. M. Lieber, Nano Lett. **3**, 149 (2003).
[3] X. F. Duan, Y. Huang, Y. Cui, J. F. Wang, and C. M. Lieber, Nature (London) **409**, 66 (2001).
[4] Y. Cui, Q. Q. Wei, H. K. Park, and C. M. Lieber, Science **293**, 1289 (2001).
[5] B. Z. Tian, X. L. Zheng, T. J. Kempa, Y. Fang, N. F. Yu, G. H. Yu, J. L. Huang, and C. M. Lieber, Nature (London) **449**, 885 (2007).
[6] R. S. Wagner and W. C. Ellis, Appl. Phys. Lett. **4**, 89 (1964).
[7] P. J. A. Sazio, A. Amezcua-Correa, C. E. Finlayson, J. R. Hayes, T. J. Scheidemantel, N. F. Baril, B. R. Jackson, D. J. Won, F. Zhang, E. R. Margine, V. Gopalan, V. H. Crespi, and J. V. Badding, Science **311**, 1583 (2006).
[8] H. K. Tyagi, M. A. Schmidt, L. P. Sempere, and P. S. J. Russell, Opt. Express **16**, 17227 (2008).
[9] X. J. Zhang, Z. Ma, Z. Y. Yuan, and M. Su, Adv. Mater. **20**, 1310 (2008).
[10] J. Ballato, T. Hawkins, P. Foy, R. Stolen, B. Kokuoz, M. Ellison, C. McMillen, J. Reppert, A. M. Rao, M. Daw, S. R. Sharma, R. Shori, O. Stafsudd, R. R. Rice, and D. R. Powers, Opt. Express **16**, 18675 (2008).
[11] D. S. Deng, N. D. Orf, A. F. Abouraddy, A. M. Stolyarov, J. D. Joannopoulos, H. A. Stone, and Y. Fink, Nano Lett. **8**, 4265 (2008).
[12] S. Danto (unpublished).
[13] R. A. Zingaro and W. C. Cooper, *Selenium* (Van Nostrand Reinhold, New York, 1974).
[14] A. F. Abouraddy, M. Bayindir, G. Benoit, S. D. Hart, K. Kuriki, N. Orf, O. Shapira, F. Sorin, B. Temelkuran, and Y. Fink, Nature Mater. **6**, 336 (2007).
[15] J. S. Im, H. J. Kim, and M. O. Thompson, Appl. Phys. Lett. **63**, 1969 (1993).
[16] F. Boer, Philips Res. Rep. **2**, 352 (1947).
[17] E. J. Menke, M. A. Thompson, C. Xiang, L. C. Yang, and R. M. Penner, Nature Mater. **5**, 914 (2006).
[18] J. L. Hartke, Phys. Rev. **125**, 1177 (1962).
[19] M. Law, H. Kind, B. Messer, F. Kim, and P. D. Yang, Angew. Chem. Int. Ed. **41**, 2405 (2002).
[20] M. Wuttig and N. Yamada, Nature Mater. **6**, 824 (2007).